PERFORMANCE EVALUATION OF SPECTRAL-SPLITTING HYBRID PHOTOVOLTAIC-THERMAL SOLAR COLLECTORS

Zihao Li, Gan Huang, Christos N. Markides*

Clean Energy Processes (CEP) Laboratory, Department of Chemical Engineering,
Imperial College London, London SW7 2AZ, United Kingdom

ABSTRACT

Spectrum splitting is a promising methodology for full-spectrum solar energy utilisation, capable of improving the performance of hybrid photovoltaic-thermal solar collectors. In this study, a 3-D numerical model of an absorptive-based spectral-splitting hybrid photovoltaic-thermal (SSPVT) collector is developed, validated and used to investigate the performance of this type of solar collector. Compared to conventional PV-T collectors, which have a thermal absorber attached below a PV panel, the proposed SSPVT collector has a spectral-splitting channel placed above the PV panel. The liquid flowing through the spectral-splitting channel acts as both an optical filter and heat transfer fluid. The electrically unusable part of the solar spectrum is selectively absorbed by the liquid optical filter, thereby reducing unnecessary heat generation in the PV model. The model of the collector has been validated against experimental data with relative deviations below 3%. The electrical efficiency of such SSPVT collectors varies from 12.2% to 14.4%, while their thermal efficiency varies from 11.8% to 62.1% when the reduced temperature changes from 0.035 to 0.004.

1. INTRODUCTION

Solar energy is one of the most abundant renewable and sustainable energy sources. One of the most widespread technologies that rely on harnessing solar power is photovoltaics (PV), which can directly convert solar energy into electricity. However, regardless of the material, PV cells and modules are only sensitive to a part of the solar spectrum. For example, the theoretical electrical efficiency limit of typical single-junction silicon (Si) cells is approximately 30% [1]. The remaining wavelengths cannot be used by the cells and thus absorbed, thus elevating their temperature and ultimately losing as waste heat from the PV surface. In particular, Oh et al. [2] found that poorly ventilated PV panels can reach temperatures as high as 90 °C in hot climatic conditions.

Of importance in this context is the fact that the electrical conversion efficiency of PV cells degrades at progressively higher temperatures; for example, the efficiency of a typical crystalline Si cell has been observed to deteriorate by 6.5% for every 10 °C increase in its temperature [3]. This has motivated the development of hybrid photovoltaic-thermal (PV-T) technology, which is considered an alternative to conventional PV panels and solar thermal collectors. It integrates a thermal absorber into its design in thermal contact with the PV cells harvest residual waste heat into a useful thermal output. This delivery of a dual-energy output lends this technology a significantly higher overall (electrical plus thermal) efficiency compared to standalone PV panels and solar-thermal collectors [4–7].

Selectively-absorptive spectral splitting is a promising methodology for promoting the performance of PV-T collectors via absorbing the electrically unusable part of the solar spectrum before this reaches the PV cells, only allowing the usable fraction of the spectrum to pass through to the PV cells for electricity generation [8–11]. Despite its promising potential, limited research has been conducted on the performance evaluation of SSPVT technology. In the present study, a comprehensive 3-D model of SSPVT collectors is developed and validated against experimental data, aiming to provide an insightful evaluation of the performance of such collectors under various operating conditions and ambient conditions, *i.e.*, different mass flow rates, inlet fluid temperatures and solar irradiances.

*Corresponding Author: c.markides@imperial.ac.uk

2. METHODOLOGY

The structure of the absorptive-based non-concentrating SSPVT collector considered in this study is presented in Figure 1. The collector comprises (from top to bottom): (1) a high-transmittance glass cover, (2) a cooling channel through which a suitable spectral-splitting fluid flows, (3) an encapsulated PV module, and (4) a thermal insulation layer. The encapsulated PV module is composed of a tempered glass, encapsulant films (ethylene-vinyl acetate), monocrystalline silicon (c-Si) cells, and a back sheet (Tedlar).

In this design, the flowing fluid acts as an optical filter that is selectively absorbing a part of the electrically unusable solar spectrum. The fluid is also able to remove the heat generated in the PV module. The fluid is expected to have high transmittance in the electrically sensitive waveband of the PV cells and be able to selectively absorb the rest of the spectrum, thus reducing unnecessary heat generation in PV cells without compromising the electrical efficiency. The PV module in this study consists of c-Si PV cells, which is electrically sensitive to the wavelength of 300-1200 nm [12].

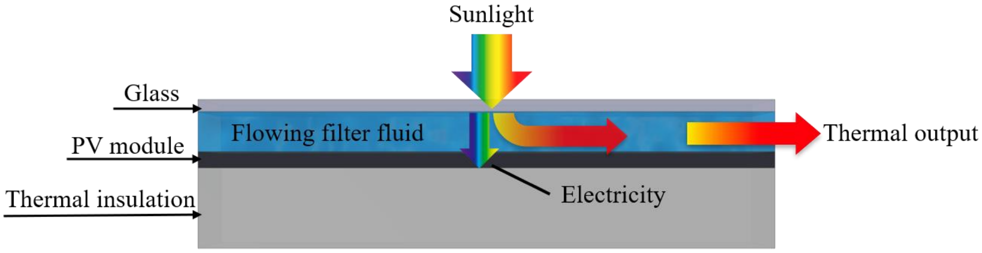

Figure 1: Schematic of selectively-absorptive SSPVT collector.

As shown in Figure 2, a liquid water layer with 10 mm thickness has high transmittance in the wavelength range of 300-1200 nm and high absorptivity in the infrared regions of the solar spectrum (*i.e.*, electrically-unusable spectrum for c-Si cells) [13]. In addition, water also has some excellent thermophysical properties working as HTF, such as a high thermal conductivity of 0.608 W/m·K, a high specific heat capacity of 4.18 kJ/kg·K and a low viscosity of 0.889 mN·s/m^2 at 25 °C [14]. Furthermore, water is stable, non-toxic and low-cost. Therefore, water is selected as the working fluid for the SSPVT collector in this study.

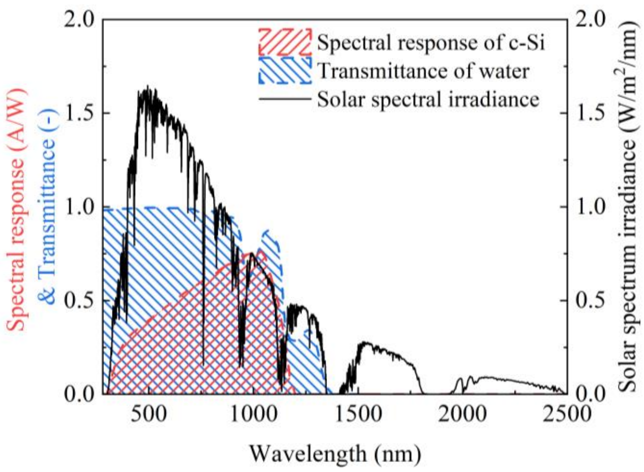

Figure 2: Spectral response of c-Si cells and optical transmittance of water with 10 mm thickness.

A three-dimensional steady-state model of the proposed SSPVT collector, featuring coupled heat transfer, fluid dynamic, optical and solar cell sub-models, was developed in COMSOL. The numerical model is based on the following assumptions: (1) solar irradiance and wind speed are uniforms over the collector's surface; (2) the thermophysical properties of all components except the fluid are constant; (3)

the solar spectrum absorbed by different layers of the SSPVT collector is converted into uniform internal heat sources; (4) the PV cells have a linear efficiency degradation with operating temperature; (5) the ambient temperature is uniform around the collector, and (6) heat losses from the sides of the collector are neglected. All equations are solved in COMSOL by finite element modelling (FEM).

The heat transfer module is applied to all components of the SSPVT collector. The governing equation of the heat transfer module is:

$$\rho c_{\mathrm{p}} \mathbf{u} \cdot \nabla T + \nabla \cdot (\mathbf{q} + \mathbf{q}_{\mathrm{r}}) = Q \tag{1}$$

where the first term on the left-hand side of Eq. (1) is the accumulation of internal energy in flowing fluid and the second term on the left-hand side corresponds to the heat flux by Fourier heat conduction (**q**) and Stenfen-Boltzman thermal radiation ($\mathbf{q}_{\mathrm{r}}$). The term Q on the right-hand side of Eq. (1) is the heat source. ρ, c_{p} and u are the density, heat capacity and velocity vector of the flowing fluid.

The optical module is applied to calculate the absorbed, transmitted and reflected solar energy by each layer (*i.e.*, the glass cover, flowing fluid, cover glass of PV module, and c-Si PV cells). The solar irradiance absorbed by layer i is:

$$Q_{\mathrm{abs},i} = \int_0^\infty \alpha_i(\lambda) G_i(\lambda)\, \mathrm{d}\lambda \tag{2}$$

where $\alpha_i(\lambda)$ is the absorptivity of layer i and $G_i(\lambda)$ is the spectral distribution of solar irradiance on layer i. The transmitted spectrum of layer i (also as the incident solar spectrum on layer i+1) is:

$$G_{\mathrm{trans},i} = G_{i+1} = \tau_i(\lambda) G_i(\lambda) \tag{3}$$

where $\tau_i(\lambda)$ is the transmittance of layer i. The solar spectrum for the c-Si PV cells, $G_{\mathrm{PV}}(\lambda)$, can be calculated by Eq. (3) based on layer-by-layer calculation.

The solar cell module is used to evaluate the photovoltaic efficiency (η_{el}) of solar cells under high operating temperatures. η_{el} is assumed to decrease linearly with increasing PV cells temperature, and the temperature coefficient of c-Si cells (0.0045 K^{-1}) is introduced to calculate η_{PV} [15]:

$$\eta_{\mathrm{el}} = \frac{V_{\mathrm{oc}} \cdot J_{\mathrm{sc}} \cdot FF}{G_{\mathrm{PV}} \cdot A} [1 - \beta_{\mathrm{PV}} (T_{\mathrm{PV}} - T_{\mathrm{ref}})] \tag{4}$$

where V_{oc}, J_{sc}, and FF are the open-circuit voltage, the short-circuit current and the fill factor of the cell, and they can be calculated based on references [16]. A is the area of collector and β, T_{ref} are the temperature coefficient and reference temperature (25 °C) of the cell.

The thermal efficiency of the collector at steady-state conditions is:

$$\eta_{\mathrm{th}} = \frac{\dot{m} \cdot c_{\mathrm{p}} \cdot (T_{\mathrm{out}} - T_{\mathrm{in}})}{G \cdot A} \tag{5}$$

where $\dot{m}$ and c_{p} are the mass flow rate and the specific heat capacity of the working fluid, and T_{out} is the outlet fluid temperature under a steady state.

3. RESULTS AND DISCUSSION

3.1 Model Validation

The model was first validated against experimental data, generated by a series of tests performed on a prototype collector constructed and placed on the roof of the Department of Chemical Engineering at

Imperial College London (latitude: 51.5°, longitude: -0.2°). Salient validation results are summarised in Table 1, which show a worst-case relative deviation of 3%. A slight overestimation of the thermal performance by the model would be expected, which would be attributed to the underestimation of the heat losses in the model, *e.g.*, the heat losses from the sides of the collector are neglected. The accuracy of the model is considered adequate for the purposes of the present study.

Table 1: Model validation results against experimental data.

	Model	Experiment	Relative difference %
Temperature increase, °C	33.4	32.6	2.4
Electrical and thermal efficiency, %	13.3 and 41.3	13.7 and 40.6	2.6 and 1.8

3.2 Distribution of Fluid Temperature

Figure 3 shows 2-D temperature distributions of the working fluid through the investigated SSPVT collector for different mass flow rates $\dot{m}$ through the collector. It can be observed that the working fluid is heated from a low inlet temperature (28 °C) to a higher outlet temperature, which is different in each case such that the flow rate is an effective variable with which to control this output parameter.

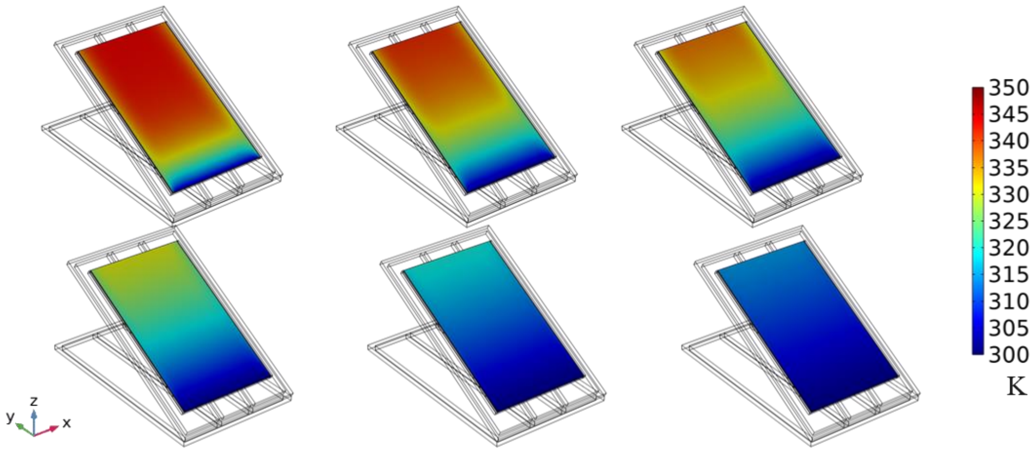

Figure 3: Distributions of fluid temperature for different fluid flow rates through the collector; first row from left to right: 3.6, 7.2 and 10.8 L/h, and second row from left to right: 18, 36 and 54 L/h.

As expected, the temperature of the delivered fluid decreases significantly as the flow rate increases, and in fact, no red region (signifying temperatures at or above ~ 60 °C) exist for a mass flow rate at or above $\dot{m}$ = 72 L/h. Of interest are the thermal boundary layers that are observed for $\dot{m}$ < 10.8 L/h, which suggests that a 3-D simulation is necessary for the accurate modelling of such collectors.

3.3 Electrical and Thermal Efficiencies

Parametric analyses have been conducted to investigate the effects of: (1) mass flow rate $\dot{m}$ (= 3.6-72 L/h), (2) inlet temperature T_{in} (= 10-60 °C), and (3) total solar irradiance G (= 500-1000 W/m^2) on the performance of the SSPVT collector. Performance curves are plotted against the reduced temperature T_r in Figure 4(a), where the reduced temperature is defined as $T_r = (T_{fm} - T_a)/G$ with T_{fm} the mean fluid temperature through the collector and T_a the ambient temperature.

According to the results in this figure, both the electrical η_{ele} and thermal η_{th} efficiencies increase from 12.2% to 14.4% and from 11.8% to 62.1%, respectively, when the reduced temperature decreases from 0.035 to 0.004. Figure 4(b) presents this variation of η_{ele} and η_{th} as a function of mass flow rate $\dot{m}$ and at a constant inlet water temperature of 28 °C. The relative increases of η_{ele} and η_{th} are 18% and 425% respectively when $\dot{m}$ increases from 3.6 to 72 L/h, which reveals that the flow rate has a more significant influence on thermal efficiency than the electrical efficiency and, as above, confirms the suitability of this variable for the control of the collector's thermal output.

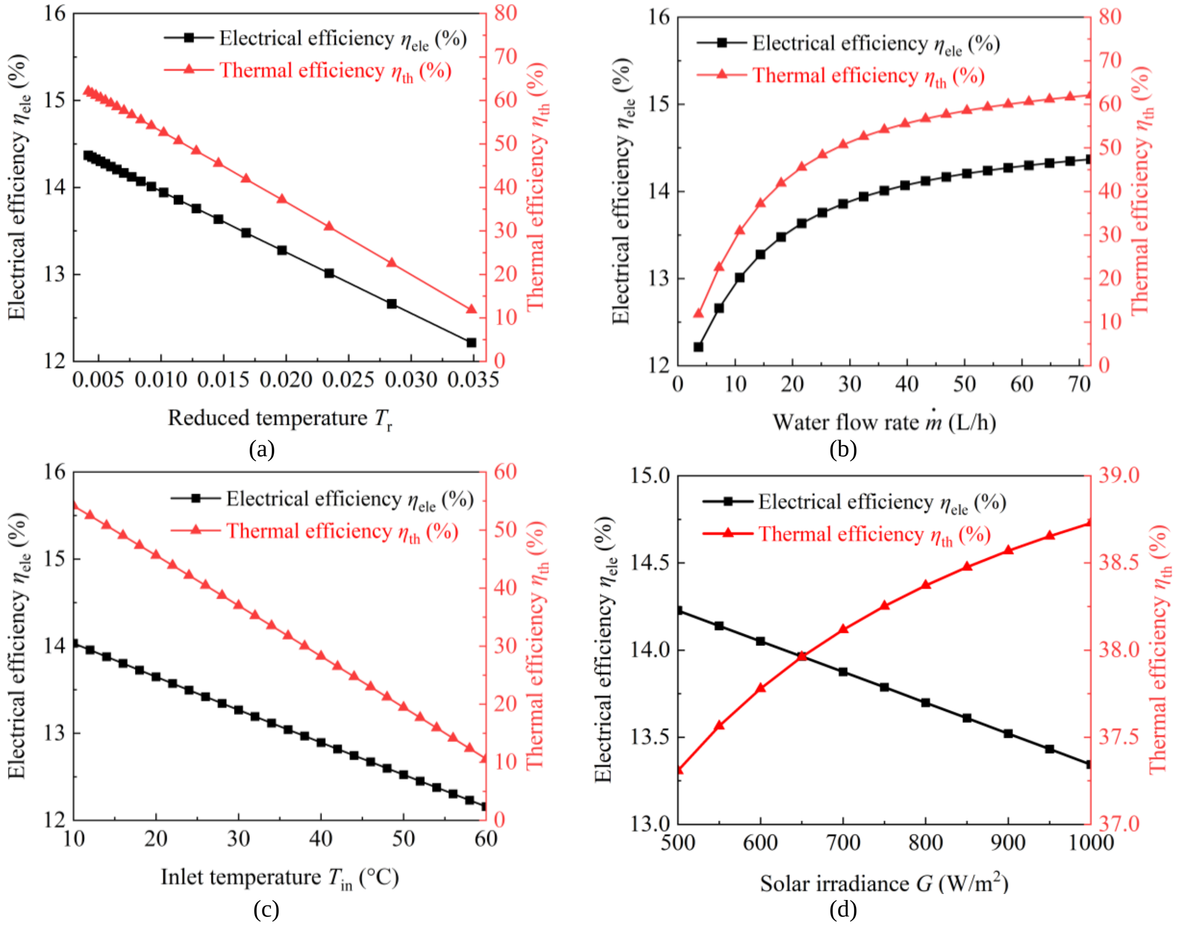

Figure 4: (a) Performance curves of the SSPVT collector, (b) variations of η_{ele} and η_{th} as a function of the water flow rate $\dot{m}$ (G = 1000 W/m^2 and T_{in} = 28 °C), (c) at different inlet temperatures T_{in} (G = 1000 W/m^2 and $\dot{m}$ = 15.4 L/h), and (d) as a function of the solar irradiance G (T_{in} = 28 °C and $\dot{m}$ = 15.4 L/h).

Figure 4(c) illustrates the effect of the inlet temperature T_{in} on the performance of the SSPVT collector at a constant flow rate of 15.4 L/h. Both η_{ele} and η_{th} linearly decrease at higher T_{in}. The mean temperature of the working fluid increases as the inlet temperature increases, resulting in a higher PV temperature and higher heat losses, which leads to a deterioration in both the electrical and thermal efficiencies of the collector. Finally, the effect of the solar irradiance G on performance (for $\dot{m}$ = 15.4 L/h and T_{in} = 28 °C) is shown in Figure 4(d). This figure shows that η_{ele} decreases from 14.2% to 13.3% with an increase of G from 500 to 1000 W/m^2 due to a higher operating temperature; on the contrary, the thermal performance improves at higher G as η_{ele} increases from 37.3% to 38.7%.

4. CONCLUSION

A comprehensive 3-D model of a spectral-splitting PV-T (SSPVT) collector has been demonstrated in this study. Parametric analyses have been conducted aimed at the performance evaluation of such a collector under various operating and ambient conditions, *i.e.*, different working fluid flow rates, inlet fluid temperatures and solar irradiances. The model has been validated against experimental data, with a worst-case relative difference of 3% between the two. The model shows that there are obvious thermal boundary layers in the temperature distribution of working fluid when the flow rate is below ~10 L/h, which indicates that it is necessary to perform 3-D simulations when modelling such collectors. According to the parametric analyses, the electrical and thermal efficiencies of the SSPVT collector increase from 12.2% to

14.4% and from 11.8% to 62.1%, respectively, when varying the reduced temperature from 0.035 to 0.004. The flow rate has a more significant influence on thermal efficiency than on electrical efficiency. It is a suitable control variable that can regulate the thermal output of the collector. Finally, a higher inlet temperature of the working fluid dramatically reduces the performance of the collector.

ACKNOWLEDGEMENTS

This work was supported by the UK Engineering and Physical Sciences Research Council (EPSRC) [grant number EP/R045518/1]. The authors would also like to thank Solar Flow Ltd. (www.solar-flow.co.uk/). Data supporting this publication can be obtained on request from cep-lab@imperial.ac.uk.

REFERENCES

[1] W. Shockley and H. J. Queisser, "Detailed balance limit of efficiency of p-n junction solar cells," *J. Appl. Phys.*, vol. 32, no. 3, pp. 510–519, Mar. 1961.

[2] J. Oh, G. Samy, and T. Mani, "Temperature testing and analysis of PV modules per ANSI/UL 1703 and IEC 61730 standards," in *Conference Record of the IEEE Photovoltaic Specialists Conference*, 2010, pp. 984–988.

[3] E. Radziemska, "The effect of temperature on the power drop in crystalline silicon solar cells," *Renew. Energy*, vol. 28, no. 1, pp. 1–12, Jan. 2003.

[4] K. Wang, M. Herrando, A. M. Pantaleo, and C. N. Markides, "Technoeconomic assessments of hybrid photovoltaic-thermal vs. conventional solar-energy systems: Case studies in heat and power provision to sports centres," *Appl. Energy*, vol. 254, p. 113657, Nov. 2019.

[5] I. Guarracino, A. Mellor, N. J. Ekins-Daukes, and C. N. Markides, "Dynamic coupled thermal-and-electrical modelling of sheet-and-tube hybrid photovoltaic/thermal (PVT) collectors," *Appl. Therm. Eng.*, vol. 101, pp. 778–795, May 2016.

[6] M. Herrando, A. Ramos, I. Zabalza, and C. N. Markides, "A comprehensive assessment of alternative absorber-exchanger designs for hybrid PVT-water collectors," *Appl. Energy*, vol. 235, pp. 1583–1602, Feb. 2019.

[7] I. Guarracino, J. Freeman, A. Ramos, S. A. Kalogirou, N. J. Ekins-Daukes, and C. N. Markides, "Systematic testing of hybrid PV-thermal (PVT) solar collectors in steady-state and dynamic outdoor conditions," *Appl. Energy*, vol. 240, pp. 1014–1030, Apr. 2019.

[8] G. Huang, S. R. Curt, K. Wang, and C. N. Markides, "Challenges and opportunities for nanomaterials in spectral splitting for high-performance hybrid solar photovoltaic-thermal applications: A review," *Nano Mater. Sci.*, vol. 2, no. 3, pp. 183–203, Sep. 2020.

[9] H. Liang, F. Wang, L. Yang, Z. Cheng, Y. Shuai, and H. Tan, "Progress in full spectrum solar energy utilisation by spectral beam splitting hybrid PV/T system," *Renewable and Sustainable Energy Reviews*, vol. 141. Elsevier Ltd, p. 110785, May 01, 2021.

[10] G. Huang, K. Wang, S. R. Curt, B. Franchetti, I. Pesmazoglou, and C. N. Markides, "On the performance of concentrating fluid-based spectral-splitting hybrid PV-thermal (PV-T) solar collectors," *Renew. Energy*, vol. 174, pp. 590–605, Aug. 2021.

[11] G. Huang, K. Wang, and C. N. Markides, "Efficiency limits of concentrating spectral-splitting hybrid photovoltaic-thermal (PV-T) solar collectors and systems," *Light Sci. Appl.*, vol. 10, no. 1, pp. 2047–7538, Dec. 2021.

[12] H. Field, "Solar cell spectral response measurement errors related to spectral band width and chopped light waveform," in *Conference Record of the IEEE Photovoltaic Specialists Conference*, 1997, pp. 471–474.

[13] X. Han, D. Xue, J. Zheng, S. M. Alelyani, and X. Chen, "Spectral characterisation of spectrally selective liquid absorption filters and exploring their effects on concentrator solar cells," *Renew. Energy*, vol. 131, pp. 938–945, Feb. 2019.

[14] T. L. Bergman, *Fundamentals of heat and mass transfer*. 2019.

[15] T. T. Chow, "Performance analysis of photovoltaic-thermal collector by explicit dynamic model," *Sol. Energy*, vol. 75, no. 2, pp. 143–152, Aug. 2003.

[16] T. Otanicar, I. Chowdhury, P. E. Phelan, and R. Prasher, "Parametric analysis of a coupled photovoltaic/thermal concentrating solar collector for electricity generation," *J. Appl. Phys.*, vol. 108, no. 11, Dec. 2010.